Available online at www.sciencedirect.com
SCIENCE DIRECT®
Journal of Solid State Chemistry 175 (2003) 284–288
JOURNAL OF SOLID STATE CHEMISTRY
http://elsevier.com/locate/jssc

Synthesis of the complex fluoride $LiBaF_3$ and optical spectroscopy properties of $LiBaF_3$:M(M = Eu,Ce) through a solvothermal process

Ruinian Hua,[b] Bingfu Lei,[a] Demin Xie,[b] and Chunshan Shi[a,*]

[a] *Key Laboratory of Rare Earth Chemistry and Physics, Changchun Institute of Applied Chemistry, Chinese Academy of Sciences, Changchun 130022, China*

[b] *Faculty of Chemistry, Northeast Normal University, Changchun 130024, China*

Received 28 March 2003; received in revised form 29 April 2003; accepted 8 May 2003

Abstract

The complex fluoride $LiBaF_3$ and $LiBaF_3$:M(M = Eu, Ce) is solvothermally synthesized at 180°C and characterized by means of X-ray powder diffraction, scanning electron microscopy, thermogravimetric analysis and infrared spectroscopy. In the solvothermal process, the solvents, molar ratios of initial mixtures and reaction temperature play important roles in the formation of products. The excitation and emission spectra of the $LiBaF_3$:M(M = Eu,Ce) have been measured by fluorescence spectrophotometer. In the $LiBaF_3$:Eu emission spectra, there is one sharp line emission located at 360 nm arising from $f \rightarrow f$ transition of Eu^{2+} in the host lattice, and typical doublet $5d-4f$ emission of Ce^{3+} in $LiBaF_3$ powder is shown.
© 2003 Elsevier Inc. All rights reserved.

Keywords: $KMgF_3$; Optical properties; Solvothermal process

1. Introduction

Since the 1970s, a number of papers [1,2] have reported the high temperature solid state syntheses of complex fluoride $LiBaF_3$ in LiF–BaF_2 system. Some complex fluorides with general formula ABF_3 (A = Li, Na, K; B = divalent metals elements) possess Perovskite structures. The complex fluoride ABF_3 have become important as it shows lasing action [3] when it is doped with a proper dopant. Various isomorphous replacements in the framework of complex fluorides lead to many controllable properties [4]. However, the solid state synthetic apparatus requires a complicated set-up because of the corrosion by fluorides. Recently, a mild hydrothermal synthesis of the complex fluorides at 120–240°C have been reported [5–8]. The contents of oxygen in ABF_3 synthesized by hydrothermal method is lower than that of the corresponding ABF_3 synthesized by high temperature solid state reaction [9]. On one hand, there are many interesting properties of the complex fluorides, such as piezoelectric characteristic [10], ferromagnetic [11], and nonmagnetic insulator behavior [12]. On the other hand, the broad UV emission from $5d-4f$ transition makes it possible to develop a tunable short-wave solid state laser [13] and amplifier [14] when doped with the rare-earth ions. In general, the luminescent properties of fluorides doped with the rare-earth ions materials synthesized by different methods have obvious difference. In order to develop new routes to synthesize complex fluorides without complicated syntheses apparatus and in the meanwhile to do research on the luminescent properties of fluorides doped with rare-earth ions, herein we report a convenient solvothermal synthesis of $LiBaF_3$ and $LiBaF_3$:M (M = Eu,Ce) with Perovskite structure.

2. Experimental

2.1. Preparation of $LiBaF_3$ and $LiBaF_3$:M (M=Eu,Ce)

Synthesis of $LiBaF_3$ powder was carried out in a 20 mL Teflon-lined stainless steel autoclave under autogenous pressure. The starting reactants were LiF (A.R.) and BaF_2 (A.R.). The molar ratios of initial mixtures were 1.0LiF:1.0BaF_2. The typical synthesis procedure was as follows: 0.130 g LiF and 0.877 g BaF_2 were mixed and added into a Teflon-lined autoclave. Then the autoclave was filled with ethylene glycol up to

*Corresponding author. Fax: 86-0431-568-5653.
E-mail address: cshi@ciac.jl.cn (C. Shi).

0022-4596/03/$ - see front matter © 2003 Elsevier Inc. All rights reserved.
doi:10.1016/S0022-4596(03)00282-2

80% of the total volume. The autoclave was sealed into a stainless steel tank and heated in an oven at 180°C for 2 days. After being cooled to room temperature naturally, the final powder products were filtered off, washed with absolute ethanol and distilled water, and then dried in air at ambient temperature. For the synthesis of $LiBaF_3$:M (M = Eu,Ce), the mole ratios of initial mixtures were 1.0LiF:1.0BaF_2:0.02MF_3, 1.0LiF:1.0BaF_2:0.04MF_3, 1.0LiF:1.0BaF_2:0.06MF_3, 1.0LiF:1.0BaF_2:0.08MF_3 and 1.0LiF:1.0BaF_2:0.10MF_3. The other operations are the same as the synthesis process of $LiBaF_3$.

2.2. Characterization of products

All products were characterized by X-ray powder diffraction(XRD), using a Japan Rigaku D/max-IIB diffractometer with Cu$K\alpha_1$ radiation ($\lambda = 0.1541$ nm). The XRD data for index and cell-parameter calculations were collected by a scanning mode with a step of 0.02° in the 2θ range from 10° to 100° and a scanning rate of 4.0° min^{-1} with silicon used as an internal standard. Observation of crystallites by SEM was performed on a Hitachi S-570 scanning electron microscopy, aurum was used to coat the particles as a means to reduce charging effects. Thermogravimetric analysis (TGA) was conducted using a DT-30 thermogravimetric system in air. IR spectra were obtained with a Magna 560 spectrometer in the range 400–4000 cm^{-1}. The samples were pressed KBr pellets for the spectral measurements. Luminescence spectra were measured using a Hitachi F-4500 fluorescence spectrometer. All measurements were carried out at room temperature.

3. Results and discussion

3.1. Synthesis conditions

Table 1 shows the solvothermal synthesis conditions for $LiBaF_3$ and $LiBaF_3$:M (M = Eu, Ce). In the synthesis of $LiBaF_3$, the Li/Ba ratio was found to be crucial to the formation, crystallization and purity of the product. When the molar ratio Li/Ba of mixture was 1, and ethylene glycol was used as a solvent, the pure and well-crystallized products were prepared. However, when the molar ratio Li/Ba was 0.5 (or 2), impurity phase BaF_2 (or LiF) appeared. The formation of highly pure $LiBaF_3$ powder also depended on the solvents. Other solvents were also employed to synthesize $LiBaF_3$, such as n-butanol, ethylenediamine, pyridine and phenol etc. The result reveals that all of the other solvents cannot form the high purity products.

Synthesis temperature was also an important factor for an effective synthesis. For instance, in the LiF–BaF_2–ethylene glycol system, $LiBaF_3$ is obtained after 1 day at 180°C, but at 150°C for 7 days cannot form the pure crystals of $LiBaF_3$. The synthesis reaction can be formulated as follows:

$$LiF + BaF_2 \xrightarrow{\text{ethylene glycol } 180^\circ C} LiBaF_3.$$

3.2. Description of the structure

The XRD patterns of the $LiBaF_3$ show that the products can be indexed in cubic system. The unit-cell parameters for $LiBaF_3$, $LiBaF_3$:Eu and $LiBaF_3$:Ce are $a = 3.9953 \pm 0.0019$ Å, $a = 3.9946 \pm 0.0016$ Å and $a = 4.0016 \pm 0.0033$ Å, respectively. These values are similar to that of the corresponding $LiBaF_3$ synthesized by solid-state reaction ($a = 3.9950$ Å) [JCPDS Card 18-0715]. The powder XRD patterns show that no detectable impurity is present.

3.3. Shape and size

The SEM observation of the product shows that the crystallites have regular morphology and this implies that the product is a pure and single phase (Fig. 1). The complex fluoride $LiBaF_3$ and $LiBaF_3$:M (M = Eu, Ce)

Table 1
Solvothermal synthesis conditions for $LiBaF_3$ and $LiBaF_3$:M (M = Eu,Ce)

Starting materials			$a:b:c$ mole ratio	Solvent	Reaction time (days)	Reaction temp. (°C)	Phases in product
a	b	c					
LiF	BaF_2		1:1	Ethylene glycol	7	180	$LiBaF_3$
LiF	BaF_2		2:1	Ethylene glycol	7	180	$LiBaF_3$ + LiF
LiF	BaF_2		1:2	Ethylene glycol	7	180	$LiBaF_3$ + BaF_2
LiF	BaF_2		1:1	Ethylene glycol	4	180	$LiBaF_3$
LiF	BaF_2		1:1	Ethylene glycol	2	180	$LiBaF_3$
LiF	BaF_2		1:1	Ethylene glycol	1	180	$LiBaF_3$
LiF	BaF_2		1:1	Ethylene glycol	1	200	$LiBaF_3$
LiF	BaF_2		1:1	Ethylene glycol	7	150	$LiBaF_3$ + BaF_2
LiF	BaF_2	EuF_3	1:1:0.10	Ethylene glycol	2	180	$LiBaF_3$:Eu
LiF	BaF_2	CeF_3	1:1:0.10	Ethylene glycol	2	180	$LiBaF_3$:Ce

crystallites have a cubic shape, and the average grain sizes are ca. 1.5, 1.0 and 1.0 μm, respectively.

3.4. Thermal analysis

The thermal stability of the $LiBaF_3$ was studied by TG-DTA analysis in air. No phase transition or mass loss was observed from 25°C up to 835°C in the system. This indicates that $LiBaF_3$ is not hydrated and stable in air. Water, or possibly hydroxyl groups, was not found to be present in powders as shown in IR spectrum by absorptions at 3445 and 1635 cm^{-1}.

3.5. Optical spectroscopy properties of $LiBaF_3$:Eu

Fig. 2 shows the emission spectrum of the $LiBaF_3$:Eu^{2+} powder. As can be seen, the overall appearance of the emission spectrum consisted of one broad emission band ranging from 370 to 500 nm. In addition, there is one sharp line emission located at 360 nm arising from $f \rightarrow f$ transition of Eu^{2+} in the host lattice and the intensity of the 360 nm emission peak increases when the Eu content increase. The concentration quenching occurs at about 8% of Eu (Fig. 4). The broad emission band can be attributed to the trace oxygen in the powder. The emission spectrum is similar to the previously reported in $KMgF_3$: Eu single crystal [2,15]. The excitation spectra of the $LiBaF_3$:Eu^{2+} powder are shown in Fig. 3 monitored at 360 emission. In addition, the excitation spectra monitored at 360 and 416 nm have the same result. From the excitation spectrum, it can be seen that there are at least five excitation peaks overlap the broad band range of 200–350 nm. The excitation peak can be accurately modeled using Gaussians as displayed in Fig. 3. The solid line is the excitation data, whereas the dash–dot lines connecting them are present at the Gaussians peaks located at 240, 256, 290, 317 and 335 nm. It should be noticed that the amplitudes of the Gaussians peaks were obtained by the line-shape fit and were not set to be equal. The 256, 290, 317 and 335 nm band can be attributed to the Eu^{2+} in the host lattice, and the 240 band results from the trace oxygen in the crystal [15]. The powder synthesized by solvothermal process is proved to have lower oxygen content compared to the other synthesized methods. It is worth noting that the emission spectra excited by the five different excitation peaks (240, 256, 290, 317 and 335 nm) have the same shape (Figs. 3 and 4).

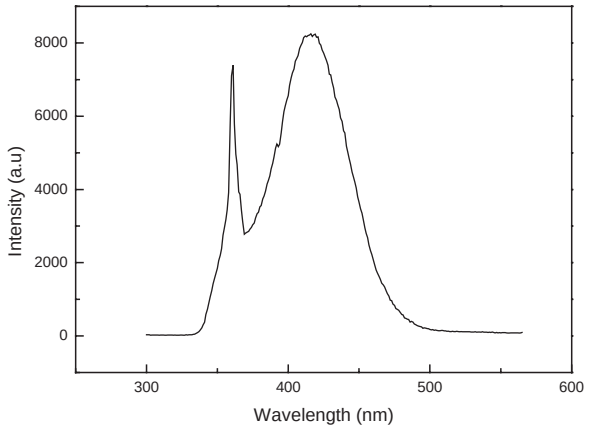

Fig. 2. The emission of $LiBaF_3$:Eu^{2+} powder excited at 290 nm.

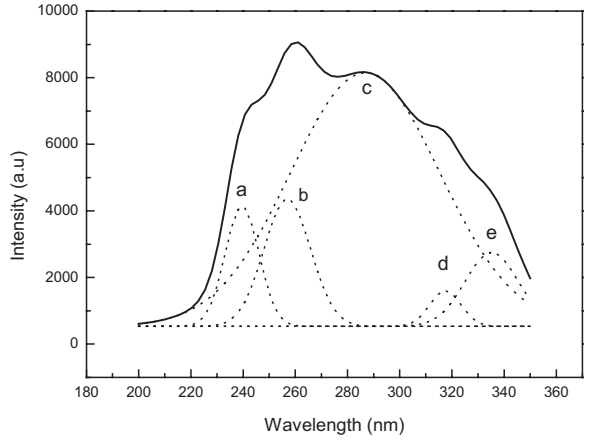

Fig. 3. The excitation of $LiBaF_3$:Eu^{2+} powder monitored at 360 nm (the excitation of $LiBaF_3$:Eu^{2+} powder monitored at 416 nm have the same result, not shown in the figure).

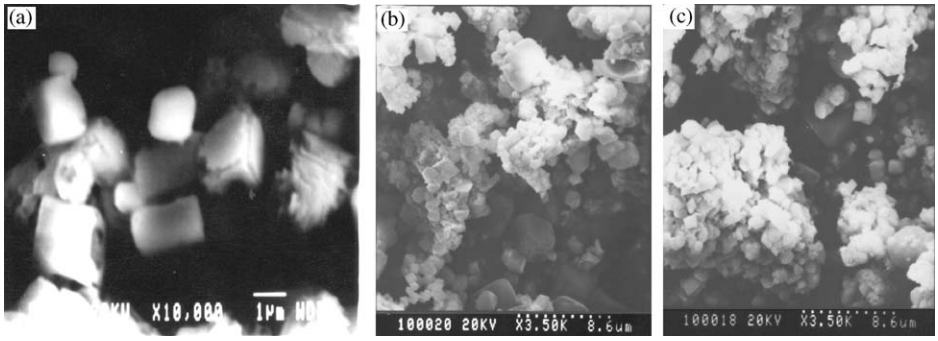

Fig. 1. SEM photographs of $LiBaF_3$ (a), $LiBaF_3$:0.10 mol Eu (b) and $LiBaF_3$:0.10 mol Ce (c).

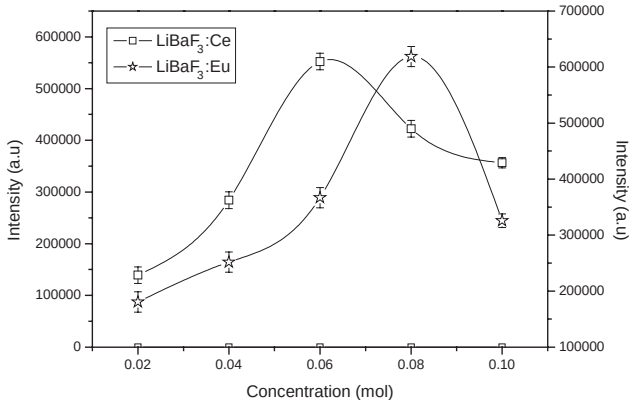

Fig. 4. The concentration of rare-earth ions dopant dependence of the fluorescence intensity.

3.6. Optical spectroscopy properties of $LiBaF_3$:Ce

The position of the $4f5d$ levels of Ce^{3+} is strongly influenced by the crystal field interaction. It is caused by a strong interaction of the $5d$-electron with the neighboring anion ligands in the compound. The typical doublet $5d-4f$ emission of Ce^{3+} in $LiBaF_3$ powder is shown in Fig. 5. The emission spectrum excited at 254 nm appear as a broad range of 290—450 nm with a maximum center located at 340 nm. The excitation spectrum for the 345 nm emission is shown in Fig. 6. There are two emission peaks in the overall range from 200 to 350 nm, located at 254 and 297 nm, respectively. This is because the $4f5d$ level of Ce^{3+} is split into at least two levels due to the crystal-field interaction of $LiBaF_3$ and the intensity of the two emission peak enhances when the Ce content increases. The fluorescence intensity of $LiBaF_3$:Ce reach it maximum when the Ce dopant is about 6% (Fig. 4). Based on the optical spectra, the $4f5d$ level position is located at about 33,600 cm^{-1} (297 nm). Due to the nonequivalent substitution, an excess of positive charge in the lattice must be compensated. The charge compensation of $LiBaF_3$ doped with Ce^{3+} has been reported by Tan [1] in detail. The conclusion drawn by Tan is that the vacancies of Li^+ ions are the favorable charge compensation pattern at low concentration of CeF_3 doped, but interstitial F^- ions are the major charge compensation pattern when the concentration of CeF_3 doped goes beyond a certain value. The fluorescence spectra of the $LiBaF_3$:Eu mentioned above revealed that there is trace oxygen in the $LiBaF_3$ matrix, so that we can infer that as the Ce^{3+} ions concentration becomes so large that it is possible to fulfil charge compensation by interstitial F^- ions and trace O^{2-}.

The differences of luminescent properties of fluorides doped with the rare-earth ions materials synthesized by solvothermal process and other methods were analyzed. The main difference of luminescent properties results from the content of oxygen in the host lattice of

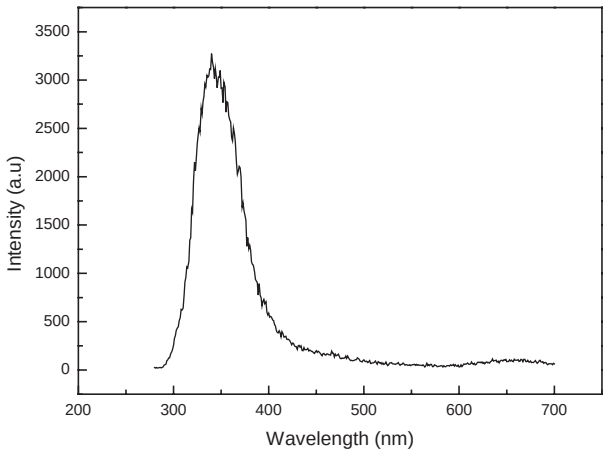

Fig. 5. The emission of $LiBaF_3:Ce^{3+}$ powder excited at 254 nm.

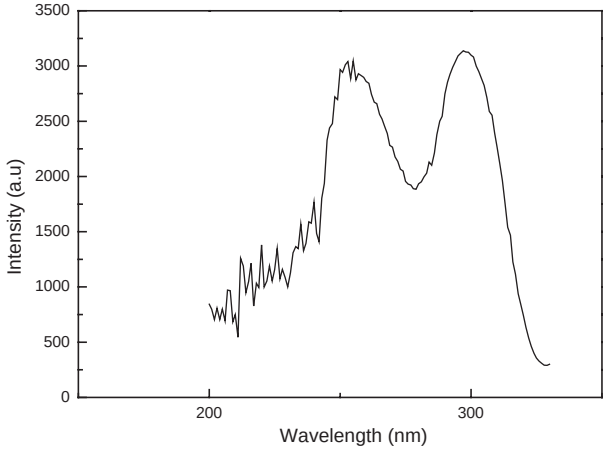

Fig. 6. The excitation of $LiBaF_3:Ce^{3+}$ powder monitored at 345 nm.

fluorides synthesized by solvothermal process. In the $LiBaF_3$:Eu emission spectra, the emission peak located at 416 nm become narrower in comparison with that of the solid state reaction at high temperature [16]. In the case of the $LiBaF_3$:Ce, its emission and excitation spectra have the same shape as that of synthesized by solvothermal process and solid state reaction, but the emission spectrum of $LiBaF_3$:Ce synthesized by solvothermal process show obvious blue shift (emission peak shift from 370 to 345 nm [16]). This blue shift can be due to the low oxygenic content in the host, and this results in the d energy level rise.

In summary, a new method for the synthesis of $LiBaF_3$ and $LiBaF_3$:M(M = Eu,Ce)by solvothermal crystallization at 180°C is presented. The solvent, molar ratios of initial mixtures and reaction temperature play important roles in the formation of the products in the solvothermal process. The products have uniform grain shapes and sizes. The product is stable in air. The excitation and emission spectra of the $LiBaF_3$: M(M = Eu,Ce) were discussed based on fluorescence spectrum. In the $LiBaF_3$:Eu emission spectra, there is

one sharp line emission located at 360 nm arising from $f \rightarrow f$ transition of Eu^{2+} in the host lattice, and typical doublet $5d-4f$ emission of Ce^{3+} in $LiBaF_3$ powder is shown. The fluorescent intensity of the $LiBaF_3$: $M(M = Eu,Ce)$ increases when the Eu and Ce contents increase, the fluorescent intensity of Ce reach maximum when Ce ions concentration is 6% and the concentration quenching occurs around 8% of Eu.

Acknowledgments

This work was supported by the State Key Project of Foundation Research (G1998061306).

References

[1] Y. Tan, C. Shi, J. Solid State Chem. 150 (2000) 178.
[2] A. Meijerink, J. Lumin. 55 (1993) 125.
[3] G. Horsch, H.J. Paus, Opt. Commun. 60 (1986) 69.
[4] K. Somaiah, M.V. Narayana, Mater. Chem. Phys. 24 (1990) 353.
[5] C. Zhao, S. Feng, Z. Chao, C. Shi, R. Xu, J. Ni, Chem. Commun. (1996) 1641.
[6] X. Xun, S. Feng, J. Wang, R. Xu, Chem. Mater. 9 (1997) 2966.
[7] C. Zhao, S. Feng, R. Xu, C. Shi, J. Ni, Chem. Commun. (1997) 945.
[8] X. Xun, S. Feng, R. Xu, Mater. Res. Bull. 33 (1998) 369.
[9] H. Li, Z. Jia, S. Feng, C. Shi, Chem. J. Chinese Univ. 12 (2000) 1805.
[10] M. Eibschutz, H.J. Guggenheim, S.H. Wemple, I. Camlibel, M. Didomenico, Phys. Lett. 7 (1969) 409.
[11] A.H. Cooke, D.A. Jones, J.F.A. Silva, M.R. Weils, J. Phys. C: Solid State Phys. 8 (1975) 4083.
[12] R.A. Heaton, C. Lin, Phys. Rev. B 25 (1982) 3538.
[13] D.J. Ehrilich, P.F. Moulton, R.M. Osgood, Opt. Lett. 4 (1979) 184.
[14] N. Sarakura, Opt. Lett. 20 (1995) 294.
[15] H. Su, Z. Jia, C. Shi, Chem. Mater. 14 (2002) 310.
[16] Y. Tan, C. Shi, J. Phys. Chem. Solids 60 (1999) 1805.